Electronic Supplementary Material (ESI) for Journal of Materials Chemistry A.

Soft while Strong Mechanical Shock Tolerable e-Skins

Yanan Wang, [ab] Baicun Hao [b], Yujia Wang [b], Yingjie Wei [b], Xin Huang [*ab] and Bi Shi [ab]

[a] National Engineering Laboratory for Clean Technology of Leather Manufacture, Sichuan University, Chengdu 610065, P.R. China.

[b] Department of Biomass Chemistry and Engineering, Sichuan University, Chengdu 610065, P.R. China. E-mail address: xhuangscu@163.com (X. Huang)

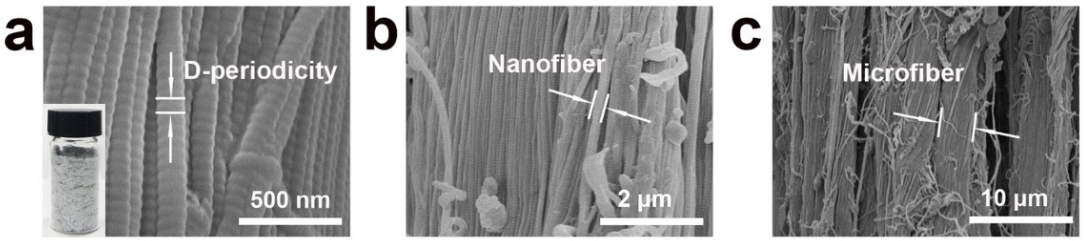

Fig. S1 FESEM images of WCFs showing (a) the D-period structure, (b) nanofibers and (c) microfibers (inset in a shows the digital photo of WCFs).

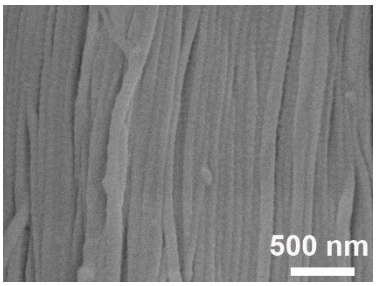

Fig. S2 FESEM image showing the microstructure of CFS-3.

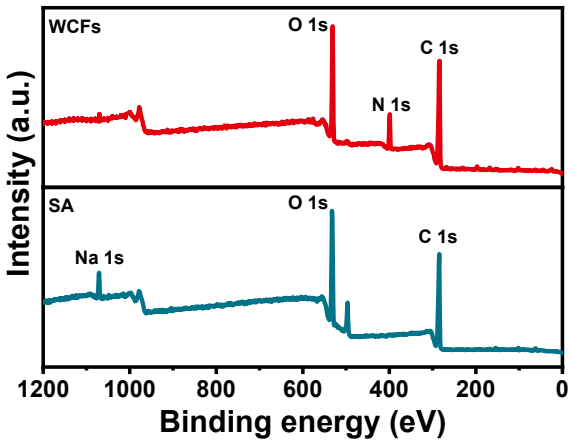

Fig. S3 XPS survey scans of WCFs and SA.

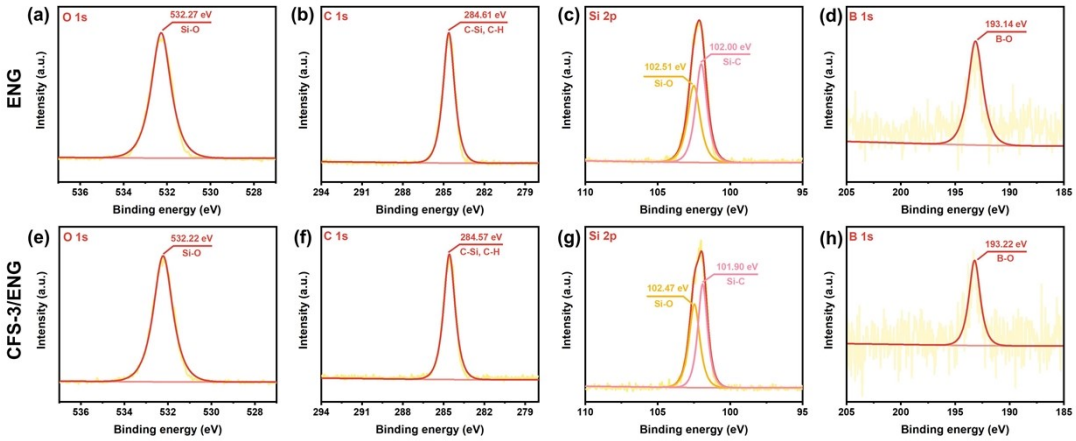

Fig. S4 O 1s, C 1s, Si 2p and B 1s XPS spectra of (a-d) ENG and (e-h) CFS-3/ENG, respectively.

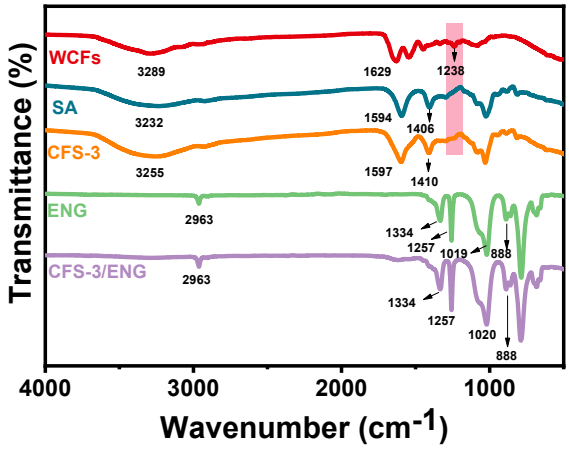

Fig. S5 FTIR spectra of WCFs, SA, CFS-3, ENG and CFS-3/ENG.

As shown in Fig. S4, the peaks at 3289, 1629 and 1238 cm^{-1} of WCFs are assigned to the stretching vibration of -OH, C=O and C-N, respectively [1]. The characteristic adsorption peaks of SA appear at 3232, 1594 and 1406 cm^{-1}, which are ascribed to the -OH, C=O and C-OH stretching bands, respectively [2]. The FTIR spectrum of CFS-3 shows the characteristic absorption peaks of SA due to the coverage of SA on WCFs. The -OH stretching vibration bands of WCFs and SA appear at 3289 cm^{-1} and 3232 cm^{-1}, respectively, while that of CFS-3 shifts to 3255 cm^{-1}, suggesting the formation of hydrogen bonding between WCFs and SA [3].

Table S1 Tensile mechanical properties of CFS-3, CFS-3/ENG, conductive CFS-3 and

conductive CFS-3/ENG.

Material	Tensile strength (MPa)	Elongation at break (%)	Toughness (MJ m^{-3})
CFS-3	0.08	6.71	0.28
CFS-3/ENG	0.20	10.6	1.00
Conductive CFS-3	0.09	4.60	0.20
Conductive CFS-3/ENG	0.22	6.34	0.65

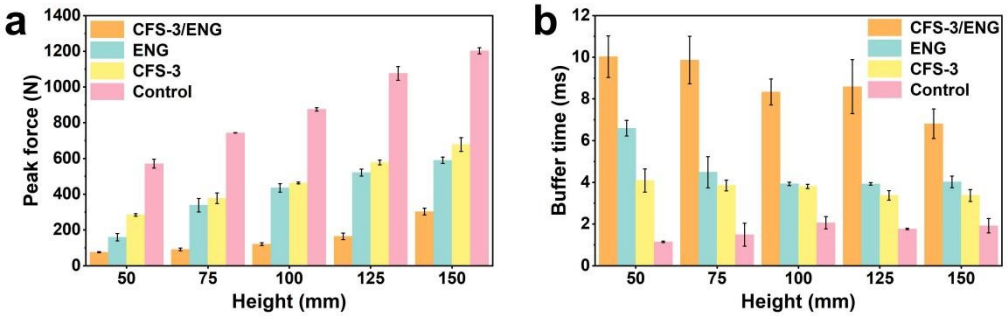

Fig. S6 The (a) peak force and (b) buffer time of control, CFS-3, ENG and CFS-3/ENG during the drop hammer tests with the drop heights of 50-150 mm.

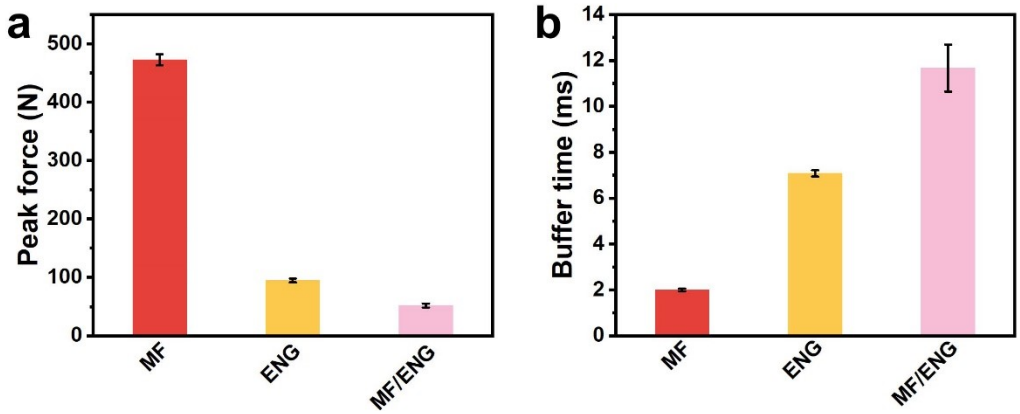

Fig. S7 (a) The peak force and (b) buffer time of MF, ENG and MF/ENG at the drop height of 50 mm.

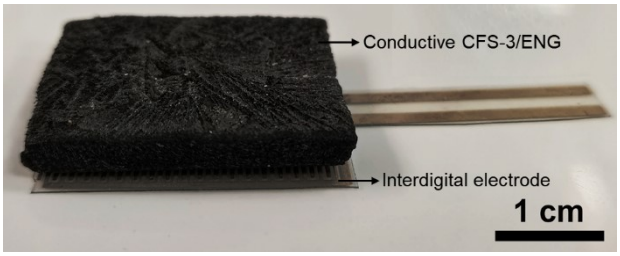

Fig. S8 The digital photo of MST e-skin.

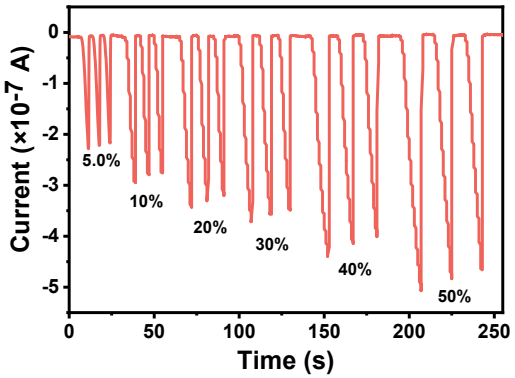

Fig. S9 *I-t* curve of MST e-skin for the detection of different mechanical deformation (5.0-50%).

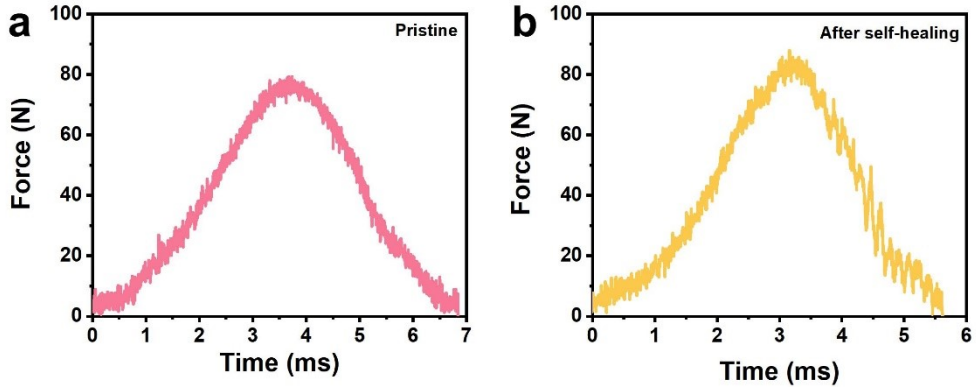

Fig. S10 The force-time curves of the (a) pristine and (b) self-healed MST e-skin during the punch by the hammer (2.36 kg) with the drop height of 20 mm.

References

[1] G. Y. Chen, Y. N. Wang, Y. J. Wang, H. Z. Xiao, X. Huang, B. Shi, *J. Mater. Chem. A* **2020**, *8*, 24388.

[2] S. K. Papageorgiou, E. P. Kouvelos, E. P. Favvas, A. A. Sapalidis, G. E. Romanos and F. K. Katsaros, *Carbohyd. Res*. **2010**, *345*, 469.

[3] Z. Wang, S. F. Hu and H. Y. Wang, *J. Food Quality* **2017**, 4954259.